Photodissociation Spectroscopy of Zn+−Formaldehyde

Wenyun Lu, Y. Abate, T.-H. Wong, and P. D. Kleiber*

Department of Physics and Astronomy, University of Iowa, Iowa City, Iowa 52242

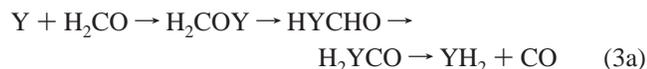*Received: July 28, 2004; In Final Form: September 20, 2004*

We report on a combined experimental and theoretical study of the photodissociation spectroscopy and chemical dynamics of Zn+−formaldehyde. We identify two overlapping absorption bands corresponding to Zn+(4s−4p)-based transitions mixed with charge-transfer character. We observe both nonreactive (Zn+ and H_2CO^+) and reactive (ZnH+ and HCO+) dissociation products. The work is supported by TD-UB3LYP level ab initio electronic structure calculations of the ground and low-lying excited energy surfaces. On the basis of the experimental and theoretical results, we propose a model for the reactive dissociation that proceeds via H-atom abstraction on the charge-transfer surface. This work shows important differences with results from previous experiments on Mg+− and Ca+−aldehyde complexes despite the similar valence character for these metal ions.

Introduction

H_2CO is the simplest aldehyde molecule, and its chemical interactions are of significant interest, both for fundamental scientific reasons and because of its importance in many applications including combustion, catalysis, atmospheric chemistry, and astrochemistry.[1,2] Gas-phase radical reactions with formaldehyde are generally thought to proceed through one of two competing mechanisms, direct H-atom abstraction, or an addition reaction involving attack on the CO π-bond, followed by C−H bond insertion and decomposition, e.g.

$$R + H_2CO \rightarrow [RHCHO] \rightarrow RH + CHO \quad (1)$$

$$R + H_2CO \rightarrow [H_2COR] \rightarrow [HRCHO] \rightarrow RH + CHO \quad (2)$$

Experimental and theoretical studies of the $O(^3P) + H_2CO$ and $OH + H_2CO$ reactions have concluded that the H-atom abstraction mechanism dominates, at least at low energies.[3−5] For $H + H_2CO$ reactions, recent experiments suggest that abstraction and addition−elimination pathways are competitive.[6] For transition-metal reactions with formaldehyde, recent crossed molecular beam studies (and subsequent ab initio modeling calculations) have found that the reaction $Y + H_2CO$ proceeds through a multistep insertion process:[7,8]

$$Y + H_2CO \rightarrow H_2COY \rightarrow HYCHO \rightarrow$$
$$H_2YCO \rightarrow YH_2 + CO \quad (3a)$$
$$\text{or} \rightarrow H_2 + YCO \quad (3b)$$

Studies of the chemical interactions of group II metal ions with H_2CO are interesting because, as with H-atoms, multiple reaction pathways might be open. In addition, Mg+− and Ca+−H_2CO chemistry may be important in the organic chemistry of the interstellar medium. Photodissociation spectroscopy of weakly bound precursor molecules M+(H_2CO) provides a valuable tool for probing chemical interactions in both ground and excited states. We recently reported on the photodissociation

spectroscopy of Mg+(3s)− and Ca+(4s)−formaldehyde complexes, M+(H_2CO), and the analogous Mg+−acetaldehyde complex, Mg+(CH_3CHO).[9−11] In each case the complex is electrostatically bound in oxygen end-on M+−O=RCH geometry, and we observe strong absorption bands that correlate with metal-based transitions, and weak formaldehyde-based ($\pi^* \leftarrow$ n) absorption bands. Nonreactive dissociation to the bare metal ion (Mg+ or Ca+) was the major product channel in both cases, although we did observe a very weak reaction to MgH+ + HCO products at high excitation energies in the Mg+ case. Here we report on a similar study of Zn+(H_2CO). While the Zn+($3d^{10}4s^1$) electronic valence is similar to that of Mg+($3s^1$) or Ca+($4s^1$), Zn+−hydrocarbon complexes often show spectroscopy and photochemical dynamics very different from those of their main-group-metal analogues.[12−14] These differences result in large part from the high ionization potential for Zn, so that metal−hydrocarbon charge-transfer channels are accessible at low energy, opening additional pathways for quenching and reaction. Indeed, here we find that charge transfer (CT) plays a major role in the dynamics, opening a pathway for efficient C−H bond activation in formaldehyde.

Additional motivation for the study of Zn interactions with formaldehyde comes from the fact that many reactions of organic carbonyl compounds (esters, amides, aldehydes, ketones) in synthetic organic chemistry and enzyme-catalyzed transformations can be catalyzed by zinc-containing metal salts or complexes.[15−17] In these reactions Zn attaches to the carbonyl oxygen to induce Lewis acidic activation, but the reaction mechanism is not fully developed.[15]

Theoretical Calculations

We have carried out a series of ab initio electronic structure calculations to investigate the ground-state bonding and interactions in the low-lying doublet excited states of Zn+−formaldehyde using Gaussian 98.[18]

Ground-State Surface. Optimization calculations at the UHF/6-311++G(d,p) and MP2/6-311++G(d,p) levels find a ground-state equilibrium for Zn+(H_2CO) with Zn bonded end-on to the O atom in a C_{2v} association complex similar to previous results for the analogous Mg+− and Ca+−formalde-

* To whom correspondence should be addressed. E-mail: paul-kleiber@uiowa.edu.

TABLE 1: Summary of the Calculated Results for the Global Equilibrium Complex I

calculation	R(Zn−O) (Å)	$\angle$(Zn−O−C) (deg)	D_e''(Zn−O) (eV)
UHF/6-311++G(d, p)	2.055	180	1.38
MP2/6-311++G(d, p)	2.051	180	1.32
UB3LYP/6-31+G(d,p)	2.084	137.5	1.533
UB3LYP/6-311++G(d, p)	2.087	140.4	1.486
UB3LYP/6-311++G(2d ,2p)	2.079	137.2	1.491
UB3LYP/6-311++G(3d f,3pd)	2.066	138.5	1.515

hyde systems (Table 1). However, a density functional theory (DFT) calculation at the UB3LYP/6-311++G(d,p) level finds the most stable ground-state complex to be bound in planar C_s symmetry with a Zn−O−C bond angle of $\angle$(ZnOC) = 140.4°. The calculated Zn−O equilibrium bond length is R(Zn−O) = 2.087 Å, with the formaldehyde ligand relatively undistorted from its isolated geometry. This ground-state equilibrium geometry is shown as structure **I** in Figure 1, with the structural parameters given explicitly in Table 2. The calculated Zn−OCH$_2$ bond dissociation energy at the UB3LYP/6-311++G(d,p) level is D_e''(Zn−O) = 1.486 eV. A frequency calculation for the ground state finds the three low-energy intermolecular vibrational mode frequencies in Zn$^+$(CH$_2$O) to be $\omega_6 = 280$ cm^{-1} for the (a′) Zn$^+$−O intermolecular stretch, $\omega_7 = 151$ cm^{-1} for the in-plane (a′) wag, and $\omega_9 = 260$ cm^{-1} for the out-of-plane (a″) wag.

Calculations carried out with a larger basis set, UB3LYP/6-311++G(3df,3pd), give results that differ only slightly: R(Zn−O) = 2.066 Å, $\angle$(ZnOC) = 138.5°, and D_e''(Zn−O) = 1.515 eV. These results are compared in Table 1. Because the differences with basis set are small, we have used the lower 6-311++G(d,p) basis for most of the calculations discussed below. These results differ qualitatively from our previous findings for Mg$^+$− and Ca$^+$−formaldehyde complexes, where the equilibrium geometry was determined both experimentally and theoretically to be C_{2v} in the ground state. Binding in Zn$^+$(H$_2$CO) appears to be more similar to that in Cu$^+$(H$_2$CO),[19] and shows substantial CT character with a ground-state Mullikin charge distribution over the heavy atoms of Zn$^{+0.7}$O$^{-0.2}$C$^{+0.5}$.

DFT calculations at the UB3LYP/6-311++G(d,p) level find two additional stable geometries (with positive definite Hessians) on the ground-state surface. The lower energy of these is also an association complex, but in an abstraction-like geometry shown as structure **II** in Figure 1 and Table 2. The abstraction complex **II** shows the Zn$^+$ weakly bonded to the H-atom in a Zn$^+$−HCHO C_s geometry with a nearly linear Zn−H−C bond ($\angle$(ZnHC) = 186.6°) and R(Zn−H) = 2.100 Å. The intermolecular vibrational mode frequencies for this structure are $\omega_6 = 100$ cm^{-1} for the (a′) Zn$^+$−O intermolecular stretch, $\omega_7 = 194$ cm^{-1} for the in-plane (a′) wag, and $\omega_9 = 298$ cm^{-1} for the out-of-plane (a″) wag (where we use the same vibrational mode numbering as above for consistency). The abstraction complex **II** lies 0.969 eV above the global minimum complex **I**, and with a bond dissociation energy to Zn$^+$ + H$_2$CO products of D_e''(Zn−H) = 0.516 eV. We have also found the transition state (TS) for passing from the global equilibrium structure **I** to the abstraction complex **II** (see Figure 1 and Table 2); the activation barrier is 1.412 eV above the global minimum, which is 0.344 eV below the Zn$^+$ + H$_2$CO asymptote. Thus, both complexes **I** and **II** can form with no activation barrier from the entrance channel, and it is possible that both ground-state association complexes may be present in our molecular beam, although we expect the more strongly bound structure **I** to be thermodynamically favored in the cold clusters from our supersonic molecular beam source. A scan of the potential
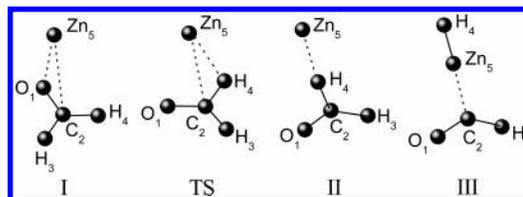
Figure 1. Complex structures for the stationary points of the [Zn,2H,C,O] ground-state surface calculated at the UB3LYP/6-311++G(d,p) level. Structural parameters are summarized in Table 2.

TABLE 2: UB3LYP/6-311++G(d,p) Structures and Energies of Zn$^+$ + H$_2$CO Stationary Points[a]

	I	TS	II	III
energy	−1893.603464	−1893.561497	−1893.567839	−1893.549149
R(O$_1$C$_2$)	1.224	1.187	1.174	1.166
R(C$_2$H$_3$)	1.097	1.103	1.104	1.116
R(C$_2$H$_4$)	1.098	1.166	1.189	3.735
R(C$_2$Zn$_5$)	3.129	2.914	3.282	2.204
$\angle$(O$_1$C$_2$H$_3$)	118.9	126.9	127.1	126.6
$\angle$(O$_1$C$_2$H$_4$)	122.3	120.2	119.8	115.6
$\angle$(O$_1$C$_2$Zn$_5$)	25.4	79.4	113.2	115.4
ω_1(a′)	3119		2968	2824
ω_2(a′)	3004		2113	1918
ω_3(a′)	1727		1876	1895
ω_4(a′)	1516		1368	1031
ω_5(a′)	1244		1101	358
ω_6(a′)	280		193	287
ω_7(a′)	151		100	180
ω_8(a″)	1236		1106	686
ω_9(a″)	260		298	309

[a] Energy in atomic units: E(Zn$^+$+H$_2$CO) = −1893.548873 au, E(ZnH$^+$+HCO) = −1893.490464 au. Bond lengths in angstroms, angles in degrees, and vibrational frequencies in inverse centimeters.

surface in the C−H bond coordinate shows there is no barrier for H-atom abstraction to ZnH$^+$ + CHO products above the reaction endoergicity; the ZnH$^+$···CHO bond dissociation energy from structure **II** is D_e''(ZnH−CHO) = 2.105 eV.

An additional stable ground-state complex is shown as structure **III** in Figure 1, and can be characterized as a HZn$^+$−CHO insertion complex. In this complex the Zn−H bond length is close to its value in isolated ZnH$^+$, R(Zn−H) = 1.530 Å, the Zn−C bond length is R(Zn−C) = 2.204 Å, and the C−Zn−H bond angle is nearly linear, $\angle$(CZnH) = 179.6°. This complex lies 1.478 eV above the global minimum structure **I** and is then essentially unbound relative to the Zn$^+$ + H$_2$CO entrance channel. Unfortunately, we have not been able to precisely locate the transition saddle point for formation of the insertion structure **III**. However, searching the parameter space suggests that the activation barrier to reach **III** is probably quite high in energy, >1 eV above the entrance channel asymptote, and it is unlikely to form in our molecular beam source. This is consistent with the fact that we observe no ZnH$^+$ coming from prereaction in the molecular beam source under typical operating conditions.

2. Excited-State Surfaces. We have used both UCIS and TD methods to study the low-lying dipole-allowed excited states of Zn(H$_2$CO)$^+$. Calculations show that the Zn$^+$-based 4p ← 4s transitions will dominate the UV absorption spectrum. There is also a very weak formaldehyde-based π^* ← n transition in the near UV. Finally, owing to the low ionization energy difference between Zn (IE = 9.394 eV) and H$_2$CO (IE = 10.88 eV), the CT state lies at very low energy and should be accessible in our experiment.

Figures 2 and 3 show UCIS/6-311++G(d,p) potential energy surfaces for the dipole-allowed doublet excited states of Zn$^+$(H$_2$CO). The solid curves of Figure 2 are rigid body scans, obtained by varying the Zn−C bond distance, keeping the

Photodissociation Spectroscopy of Zn$^+$−Formaldehyde

J. Phys. Chem. A, Vol. 108, No. 48, 2004 **10663**

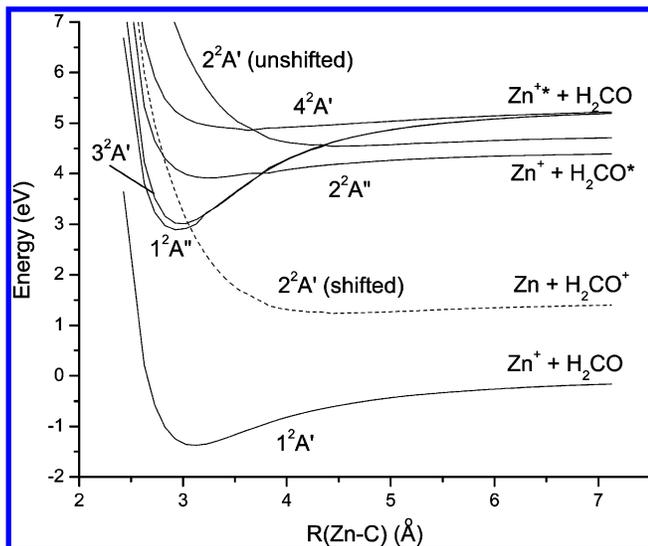**Figure 2.** Calculated potential energy curves for the low-lying doublet excited states of Zn$^+$(H$_2$CO) at the UCIS/6-311++g(d,p) level. The curves are rigid-body scans in the Zn−C coordinate, keeping all other parameters fixed at the ground-state equilibrium values ($\angle$(OCZn) = 25.4°).
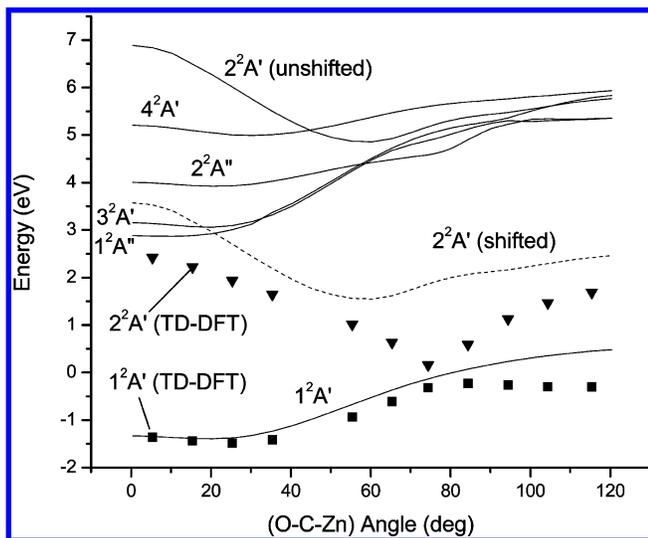

Figure 3. Calculated potential energy curves for the low-lying doublet excited states of Zn$^+$(H$_2$CO) at the UCIS/6-311++g(d,p) level. The curves are rigid-body scans in the O−C−Zn angle coordinate, keeping all other parameters fixed at the ground-state equilibrium values (R(Zn−C) = 3.129 Å). The solid points are calculated at the TD-UB3LYP/6-311++G(d,p) level for 1^{2}A′ (squares) and 2^{2}A′ (triangles), and are "unshifted" (see the text).

O−C−Zn bond angle and all other geometrical parameters fixed at the ground-state optimized values. The solid curves of Figure 3 are similar rigid body scans except the O−C−Zn bond angle is varied, with the Zn−C bond length (and all other parameters) held fixed at the ground-state equilibrium values. Results from TD-UHF calculations are essentially similar; typically these calculations agree to within ∼0.2 eV.

In previous work, we have found the CIS method can give reliable results for the metal ion based s−p transitions, but is often significantly in error for the CT excited states. We find a similar result here for both the CIS and TD-HF calculations: The asymptotic energy corrections are relatively small for the Zn$^+$(4p←4s) transitions (∼0.7 eV), but quite large for the CT state. Specifically, the calculated Zn + H$_2$CO$^+$ asymptote lies at 4.80 eV, which is 3.31 eV above the value obtained from the experimental difference in ionization energies, [IE(H$_2$CO)

− IE(Zn)] = 1.49 eV. This presents a serious difficulty in the analysis since we believe the CT state plays the dominant role in the dissociation and reaction dynamics. Nevertheless, our previous experience has shown that CIS level results can give valuable qualitative insight into the spectroscopy and dissociation dynamics if the calculated CT potential energy curves are simply shifted down to the correct asymptotic energy.[13] This has been done in Figures 2 and 3, where the CT surface, shown as the dashed line labeled 2^{2}A′, has been shifted down by 3.31 eV. This is obviously a crude approximation. To test this idea, we carried out a series of TD-DFT calculations.

Results from TD-UB3LYP/6-311++G(d,p) level calculations for the ground and CT states are shown as solid points in Figure 3. (These results are *not* "shifted".) Additional TD-DFT results will be given below. The TD-DFT points show an apparent surface crossing near $\angle$(OCZn) ≈ 75°, which is close to the geometry of the abstractive TS structure. In C_s symmetry these surfaces are both in the A′ state and will not cross. Differences with the shifted 2^{2}A′ curve from the CIS level results are apparent but not extreme. Notably, both calculations predict the complex can bend in-plane on the CT surface, from the Franck−Condon excitation geometry **I** toward the abstraction geometry **II** with no barrier. The results of Figure 3 suggest a dissociation and reaction pathway, vide infra.

The ground state of Zn$^+$(H$_2$CO) is in the 1^{2}A′ state in C_s symmetry, correlating with the ground-state asymptote Zn$^+$(4sσ) + H$_2$CO. At long range the first excited state is the (shifted) 2^{2}A′ CT state that correlates with the dissociation channel, Zn(4s^2) + H$_2$CO$^+$(^{2}B$_2$). The second excited state at long range, 2^{2}A′′, arises from the formaldehyde π* state. Excitation to this state corresponds to the formaldehyde-centered π* ← n transition and is expected to be very weak. There are three Zn$^+$*(4p)-based excited states at higher energy, 1^{2}A′′(4p$_z\pi$), 3^{2}A′(4pπ), and 4^{2}A′(4pσ), corresponding to states of different p-orbital alignments with respect to the intermolecular axis. The 4pπ states are more strongly bound than the ground state, and the corresponding Zn$^+$-based 4pπ ← 4sσ absorption bands are significantly red shifted from the Zn$^+$ atomic resonance line at 204 nm. In contrast, the 4^{2}A′(4pσ) state is less bound than the ground state, and the corresponding absorption band is blue shifted beyond our spectrally accessible region. Note that the diabatic potential energy curves of Figures 2 and 3 show a curve crossing between the metal-centered excited states and (shifted) CT states of ^{2}A′ symmetry. In the complex these states are coupled, and will show an avoided crossing in this energy range.

We have carried out UCIS/6-311++G(d,p) optimization calculations for the 3^{2}A′(4pπ) and 1^{2}A′′(4pπ) states. 1^{2}A′′ lies slightly lower in energy at the UCIS level, with T_e = 4.144 eV. The equilibrium geometry is again planar (C_s) with a slight contraction in the Zn−O bond length to R(Zn−O) = 1.886 Å, and opening of the Zn−O−C bond angle to $\angle$(ZnOC) = 154.9°. The intermolecular vibrational mode frequencies are ω_6 = 399 cm^{-1} for the (a′) Zn$^+$−O intermolecular stretch, ω_7 = 158 cm^{-1} for the in-plane (a′) wag, and ω_9 = 327 cm^{-1} for the out-of-plane (a′′) wag. 3^{2}A′ lies slightly higher in energy with T_e = 4.321 eV. The equilibrium geometry is planar (C_s) with a minimal change from the ground-state equilibrium geometry: R(Zn−O) = 1.950 Å and $\angle$(ZnOC) = 137.9°. The intermolecular mode frequencies are ω_6 = 364 cm^{-1} for the (a′) Zn$^+$−O intermolecular stretch, ω_7 = 226 cm^{-1} for the in-plane (a′) wag, and ω_9 = 393 cm^{-1} for the out-of-plane (a′′) wag.

We have also carried out single-point TD-UB3LYP/6-311++G(d,p) calculations at the UCIS-optimized excited-state geometries. These calculations find the ordering of the states

reversed with $T_e(3^2A') = 4.893$ eV and $T_e(1^2A'') = 5.149$ eV. Note that the TD-DFT calculations place the Zn^+-centered excited states roughly 0.7 eV higher in energy than the CIS results. These results will be compared with experimental data below.

Experimental Arrangement

The experimental approach has been described in several papers.[9-14] Weakly bound ion−molecule clusters, formed in a supersonic molecular beam apparatus equipped with a laser vaporization source, are probed by photodissociation spectroscopy in an angular reflectron time-of-flight mass spectrometer (TOFMS). Formaldehyde vapor is obtained by heating solid paraformaldehyde to a temperature of 150 °C. The formaldehyde vapor is then mixed to a concentration of ~2% with Ar in a mixing cylinder. The seeded gas mix is used in the pulsed gas valve at a backing pressure of 60 psi. While we have no direct information about the cluster temperature from this experiment, experiments in our laboratory on similar clusters typically show measured rotational temperatures of ~10−20 K.

From the source, the molecular beam passes through a skimmer into a differentially pumped extraction chamber where ion clusters are pulse extracted, accelerated, and mass resolved in the first leg of the TOFMS. Parent ion clusters are mass selected with a pulsed mass gate and then focused into the reflectron region of the flight tube. Clusters are probed in UV− vis spectral regions with a tunable Nd:YAG-based OPO system (Spectra Physics Pro-250 Nd:YAG-pumped MOPO-SL) equipped with nonlinear frequency mixing capabilities. The system allows essentially complete spectral coverage over the range from 215 nm to 1.8 μm with a laser bandwidth of ~0.15 cm^{-1}. Unreacted parent ions and daughter product ions are reaccelerated into the flight tube and mass-resolved in the second leg of the TOFMS in a standard tandem time-of-flight arrangement. A microchannel plate detector is used to detect ions, and the signals are collected with a digital storage scope and gated integrator.

Photodissociation action spectra are determined by normalizing the mass-resolved daughter ion signal by the parent ion signal and laser power as a function of laser photon energy. Laser power dependence studies are consistent with a one-photon dissociation process, although because of possible saturation effects for the bound−bound transitions we cannot entirely rule out multiphoton effects in the spectrum.

Experimental Results

Band Assignment. The photodissociation action spectrum for $Zn^+(H_2CO)$ covers the near-UV region from ~35000 to ~43000 cm^{-1}. We observe four major products: HCO^+, H_2CO^+, Zn^+, and ZnH^+, with HCO^+ being most abundant. Figure 4 shows the photodissociation mass spectrum at 255 nm for $Zn^+(H_2CO)$. The observed product branching ratio, HCO^+: H_2CO^+:Zn^+:ZnH^+ = 48:22:14:16, is roughly constant through the spectrum. As a result, the action spectrum for each product is similar. Figure 5 shows the action spectrum for the main product, HCO^+. Analysis of the flight time profiles of Figure 4 shows the HCO^+ mass peak to be sharp relative to the other observed daughter ion peaks. This is a clear indication that the other peaks are kinetic energy broadened but that the translational energy release in the HCO^+ channel is relatively small.

The action spectrum in Figure 5 contains two overlapping absorption bands, a structured band (showing at least two vibrational progressions) with an underlying continuum band. On the basis of the qualitative potential energy curves of Figures 2 and 3, we assign the underlying continuum to a mixed state
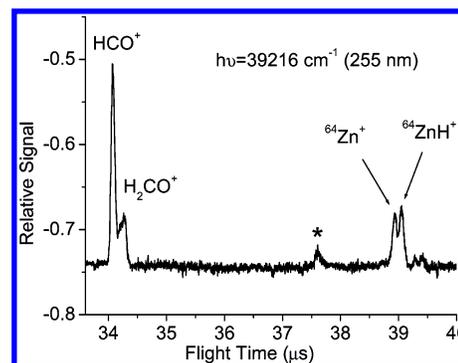

Figure 4. Photodissociation mass spectrum of $Zn^+(H_2CO)$ at 39216 cm^{-1} (255 nm). The impurity peak labeled with an asterisk comes from the cluster source and is not a dissociation product of $Zn^+(H_2CO)$.
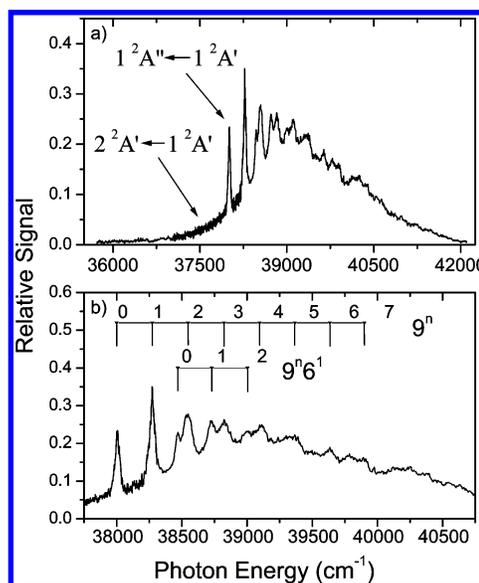

Figure 5. (a) Photodissociation action spectrum of $Zn^+(CH_2O)$, for the strongest product channel HCO^+. (b) Expanded view of the $1^2B_1 \leftarrow 1^2A_1$ band of $Zn^+(H_2CO)$ with the proposed vibrational assignment.

of $^2A'$ symmetry (with an admixture of $Zn^+(4p\pi)$ and charge-transfer character). This state is expected to dissociate rapidly with significant branching to charge-transfer-based products, as observed. We then assign the vibrationally structured state as $1^2A''$, corresponding to a $Zn^+(4p\pi)$-based excited state with the p_z-orbital lying perpendicular to the plane of the complex. At higher energies ($E > 39000$ cm^{-1}) it is unclear how much of the absorption may be due to the underlying continuum band, and how much to unresolved vibrational structure of the overlying structured band.

Vibrational Analysis of the $1^2A''(4p\pi) \leftarrow 1^2A'(4s\sigma)$ Band of $Zn^+(CH_2O)$. An expanded view of the $1^2A''(4p\pi) \leftarrow 1^2A'(4s\sigma)$ band is shown in Figure 5b. There are at least two vibrational progressions built on an obvious origin peak at 0_0^0 = 38000 cm^{-1}. The origin peak at 38000 cm^{-1} gives a vertical excitation energy for the $1^2A''(4p\pi) \leftarrow 1^2A'(4s\sigma)$ transition of 4.711 eV, which lies roughly midway between the CIS-predicted value of 4.382 eV and the TD-DFT value of 5.259 eV for this transition.

The vibrational resonance peaks are quite broad; the origin peak has a full width at half-maximum (fwhm) of ~45 cm^{-1}, and no rotational substructure is apparent. There is an obvious long progression with a spacing of about 270 cm^{-1} built on the origin. This progression is tentatively assigned to the ν_9 intermolecular out-of-plane wagging motion (a''). Birge−Sponer analysis gives the fundamental frequency ω_e = 277.3 ± 1.7

Photodissociation Spectroscopy of Zn$^+$−Formaldehyde

J. Phys. Chem. A, Vol. 108, No. 48, 2004 **10665**

TABLE 3: Vibrational Assignment for the $1^2B_1 \leftarrow 1^2A_1$ Band of Zn$^+$(H$_2$CO)

resonance (cm^{-1})	assign-ment[a]	resonance (cm^{-1})	assign-ment[a]	resonance (cm^{-1})	assign-ment[a]
38000	0^0	38730	9^16^1	39366	9^5
38273	9^1	38823	9^3	39635	9^6
38470	6^1	39903	9^26^1	39900	9^7
38548	9^2	39096	9^4		

[a] All transitions are from the $\nu'' = 0$ level of the ground state. $\nu_9 =$ Zn−O−C out-of-plane (a″) wag. $\nu_6 =$ Zn−O (a′) stretch.

cm^{-1} with an anharmonicity, $\omega_e x_e = 1.5 \pm 0.2$ cm^{-1}, for the intermolecular out-of-plane wag in $1^2A''$, which is in reasonable agreement with the predicted frequency of 327 cm^{-1} for this state. There is an additional short progression in the ν_9 vibration built on an origin peak at 38470 ($= 0_0^0 + 470$) cm^{-1}. This peak is assigned to one quantum of the ν_6 intermolecular stretch mode (a′). This result agrees passably well with the predicted value for the intermolecular stretch motion of 399 cm^{-1}. There may be higher energy modes excited as well, although at higher energies the vibrational structure is unresolved. The vibrational assignment, summarized in Table 3, should be considered as tentative. Isotope substitution experiments could resolve this uncertainty but are difficult to carry out in our experimental arrangement.

The proposed vibrational assignment in $1^2A''$ presumes an out-of-plane distortion to C_1 symmetry that is not predicted by calculations at the CIS level. While this assumption is somewhat speculative, it is consistent with previous observations in Mg$^+$(H$_2$CO) where photoexcitation of the analogous Mg$^+(3p\pi)$ state resulted in strong excitation of a″ out-of-plane vibrational modes. Out-of-plane distortion could be expected through mixing with the H$_2$CO(π^*) state (also A″); excitation of the π^* state in isolated formaldehyde is known to lead to a significant weakening of the C=O bond and an out-of-plane pyramidalization of formaldehyde. It is clear that vibronic coupling must be important since CT dissociation on the $2^2A'$ surface is a major quenching pathway from this state.

Discussion

There are several interesting observations in this work that require some discussion. Why are the action spectra similar for the different products, or in other words, why is product branching apparently independent of the excited state? Why is the major product branching to HCO$^+$, a relatively high energy product channel? Why is the branching to the lowest energy product channel Zn$^+$ so low? Why is the kinetic energy release in the HCO$^+$ product channel so small, relative to the energy release in the other channels?

The observation of the strong branching to HCO$^+$ and H$_2$CO$^+$ products indicates the importance of CT photochemistry in Zn$^+$−formaldehyde. On the basis of our ab initio calculations, we can explain these observations with reference to the energy diagram shown in Figure 6, which gives the stationary points on the Zn$^+$(H$_2$CO) potential energy surfaces calculated at the TD-UB3LYP/6-311++G(d,p) level.

Photoexcitation from the global minimum **I** is primarily to the Zn$^+$-based excited states $1^2A''$ and $3^2A'$. The bands overlap with similar experimental photoexcitation energies of $\sim$38000 cm^{-1} or 4.711 eV. The TD-UB3LYP vertical excitation energies from the global minimum **I**, $\Delta E(1^2A'') = 5.259$ eV and $\Delta E(3^2A') = 5.092$ eV, *over*estimate the experimental transition energies by $\sim$0.5 eV. The UCIS calculations *under*estimate these by $\sim$0.4 eV. Following excitation, the excited-state complexes relax toward their equilibrium geometries.
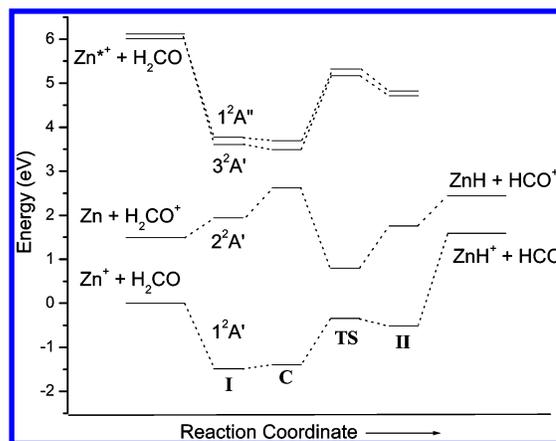

Figure 6. Reaction coordinate diagram showing the stationary points on the ground potential energy surface and the proposed reaction mechanism. The points are calculated at the TD-UB3LYP/6-311++G-(d,p) level. Structural parameters for structures **I**, **II**, and TS are given in Figure 1 and Table 2. The coupling region C is presumed to be near the excited-state minima; the point shown here corresponds to the $3^2A'$ state minimum as discussed in the text.

We propose that dissociation occurs through coupling from the metal-centered excited states to the CT surface near the region of Franck−Condon excitation in the complex. The point labeled "C" in Figure 6 corresponds to the optimized geometry for the $3^2A'$ state, which we presume to be near the coupling region. Unfortunately, the TD level calculations show a rather large energy gap at this geometry. However, we know from the vertical excitation energies that the TD-predicted Zn$^+$ excited states lie too high in energy by $\sim$0.5 eV. Charge-transfer transitions are theoretically difficult to handle, and it is also possible that the predicted CT energy is too low in this region. While we do not know exactly where the coupling occurs, we do know that efficient coupling to the CT surface must happen since H$_2$CO$^+$ and HCO$^+$ are the major dissociation products in the experiment. Coupling from $3A'(4p\pi)$ to $2A'$ is likely to be direct and efficient because the surfaces are of the same symmetry. Coupling from $1A''(4p\pi)$ to $2A'$ is indirect but may be efficient; it may occur through vibronic coupling involving the a″ out-of-plane wagging motion or through a twist (or internal rotation) of the H-atoms out of the symmetry plane. In either case the symmetry reduces to C_1 and all of the states can couple. If vibronic coupling is efficient, the vibrational resonances will be homogeneously broadened and the broadening should increase with vibrational energy in the excited states, as we observe. The final product distribution is then determined by the dissociative branching on the CT surface, independent of the initially excited state.

On the CT surface the complex can dissociate directly, breaking the Zn−H$_2$CO bond (as in Figures 2 and 6) and leading adiabatically to Zn + H$_2$CO$^+$ products. This direct process probably occurs with minimal energy redistribution into internal degrees of freedom, with most of the available energy partitioned into translation. It is possible that some of the observed HCO$^+$ product might be formed by subsequent dissociation of internally excited H$_2$CO$^+$, but our observations (translationally hot H$_2$CO$^+$ but translationally cold HCO$^+$) suggest that should be a minor process.

Figures 3 and 6 suggest a second possible dissociation route from the excited complex. Following excitation and coupling to the CT surface, the complex can bend in-plane on the CT surface, $2^2A'$, passing through the TS and abstraction geometry **II**, and adiabatically on to ZnH + HCO$^+$ products with no barrier on the CT surface. Our experimental results suggest this

Lu et al.

to be the primary dissociation pathway. The HCO$^+$ product is translationally cool, since the reaction exoergicity in this channel is small, and there is likely to be significant energy partitioning into internal rotational and vibrational modes in this abstraction process.

The branching between major product channels, HCO$^+$ and H$_2$CO$^+$, is then determined by the local forces and torques on the CT surface in the coupling region, which lead to a microscopic branching on the surface into the different product channels. The minor product channels, ZnH$^+$ and Zn$^+$, probably result from nonabiabatic coupling back to the ground-state surface. The TD-DFT calculations in Figure 3 suggest a region in the bent complex ($\angle$(OCZn) $\approx$ 75°) where such a transition can occur. Coupling to the ground-state surface can yield ZnH$^+$ + HCO, possibly with enough vibrational energy to break the Zn$-$H bond. Alternatively, Zn$^+$ might be formed by coupling to the 2^{2}A″ surface, dissociating to Zn$^+$ + H$_2$CO*.

Of course, the chemistry of formaldehyde (particularly in excited states) can be complicated. We cannot rule out that other processes could conceivably play some role in the chemical dynamics of Zn$^+$(H$_2$CO). For example, it is possible that some of the HCO$^+$ product might result from photodissociation of the stable abstraction complex **II** formed in the source. However, since that complex is relatively weakly bound, it is unlikely to be the primary source for HCO$^+$, which is the major dissociation product. It is also possible that nonadiabatic coupling from the CT surface to the ground state may allow access to the C$-$H bond insertion reaction pathway through structure **III**. In addition, while we have ignored the excited quartet states in the discussion, some weak spin$-$orbit coupling to quartet states cannot be ruled out. However, we have no reason to believe that spin$-$orbit coupling plays a major role; rather our observations are consistent with the proposed dissociation model that involves only the spin-doublet states. Finally, relaxation to the H$_2$CO(π*) surfaces could open additional pathways for C$-$H bond breaking; the unimolecular dissociation of H$_2$CO(π*) has been well studied experimentally and theoretically.[20-23]

Faced with all of these potential complications, we have chosen to invoke the principle of Occam's razor; we believe the simplest explanation that is consistent with our data is that efficient coupling to the CT surface in Zn$^+$(H$_2$CO) leads to both the soft chemical (direct CT dissociation) and hard chemical (C$-$H bond-breaking) dissociation channels. The reactive dissociation channel is efficient, probably occurring adiabatically through direct H-atom abstraction on the CT surface as suggested in Figure 6.

Photodissociation spectroscopy of Zn$^+$$-$formaldehyde complexes shows behavior markedly different from our previous observations in the Mg$^+$$-$ and Ca$^+$$-$aldehyde clusters.[9-11] These differences result primarily from the accessible low-energy CT surface in the Zn$^+$$-$formaldehyde case that opens a direct adiabatic pathway to dissociation and reaction. It is possible that the weak reaction channel previously observed at high energies in our experiments on Mg$^+$(H$_2$CO) might result from a similar CT-induced process. We plan additional calculations to investigate this possibility.

There is also an important difference in the spectroscopy of the metal ion based excited p states of A″ character. The Mg$^+$$-$formaldehyde metal ion based A″(3p) excited states appear much more strongly coupled to the π* formaldehyde based excited states. In end-on Mg$-$O approach geometry there is good spatial overlap between these molecular orbitals that facilitates transfer of electron density into the carbonyl anti-bonding orbital, resulting in a weakening of the C=O bond and formation of a partial Mg$-$O bond. This coupling leads to a major out-of-plane distortion of the complex and very high vibrational excitation in the out-of-plane wagging and C=O stretch modes. In contrast, in the Zn$^+$$-$aldehyde complex studied here, there appears to be much less distortion and, correspondingly, much weaker vibrational excitation in the analogous Zn$^+$-based A″(4p) excited state. This weaker coupling may result from less efficient spatial overlap between the p and π* molecular orbitals in the bent geometry of the Zn complex. In addition, there may be a narrower energy gap between the interacting orbitals in the Mg$^+$ case.

References and Notes

(1) Atkinson, R.; Baulch, D. L.; Cox, R. A.; Hampson, R. F.; Kerr, J. A.; Troe, J. *J. Phys. Chem. Ref. Data* **1992**, *21*, 1125.

(2) Moore, C. B.; Weisshaar, J. C. *Annu. Rev. Phys. Chem.* **1983**, *34*, 525.

(3) Klemm, R. B. *J. Chem. Phys.* **1979**, *71*, 1987. Klemm, R. B.; Skolnik, E. G. Michael, J. V. *J. Chem. Phys.* **1980**, *72*, 1256.

(4) Dupuis, M.; Lester, W. A. *J. Chem. Phys.* **1984**, *81*, 847. Dupuis, M.; Lester, W. A. *J. Chem. Phys.* **1984**, *80*, 4193.

(5) Ferrieri, R. A.; Wolf, A. P. *J. Phys. Chem.* **1992**, *96*, 7164.

(6) Oehlers, C.; Wagner, H. G.; Ziemer, H.; Temps, F.; Dobe, S. *J. Phys. Chem. A* **2000**, *104*, 10500.

(7) Stauffer, H.; Hinrichs, R. Z.; Schroden, J. J.; Floyd-Davis, H. *J. Chem. Phys.* **1999**, *111*, 10758.

(8) Bayse, C. A. *J. Phys. Chem. A* **2002**, *106*, 4226.

(9) Lu, W.-Y.; Wong, T.-H.; Sheng, Y.; Kleiber, P. D. *J. Chem. Phys.* **2002**, *117*, 6970. Lu, W.-Y.; Wong, T.-H.; Sheng, Y.; Kleiber, P. D. *J. Chem. Phys.* **2003**, *118*, 5267.

(10) Lu, W.-Y.; Kleiber, P. D. *J. Chem. Phys.* **2001**, *114*, 10288.

(11) Lu, W.-Y.; Wong, T.-H.; Sheng, Y.; Kleiber, P. D. *J. Chem. Phys.* **2003**, *118*, 6905.

(12) Lu, W.-Y.; Wong, T.-H.; Kleiber, P. D. *Chem. Phys. Lett.* **2001**, *347*, 183.

(13) Lu, W.-Y.; Kleiber, P. D.; Young, M. A.; Yang, K.-H. *J. Chem. Phys.* **2001**, *115*, 5823.

(14) Lu, W.-Y.; Wong, T.-H.; Kleiber, P. D. *J. Phys. Chem. A.* **2003**, *107*, 984.

(15) Muller, B.; Vahrenkamp, H. *Eur. J. Inorg. Chem.* **1999**, *1*, 117.

(16) *Comprehensive Organic Synthesis*; Trost, B. M., Fleming, I., Schrelber, S. L., Eds.; Pergamon Press: Oxford, 1991. Elschenbroich, C.; Slazer, A. *Organometallic Chemistry*; Teubner: Stuttgart, Germany, 1994.

(17) Frausto da Silva, J. J. R.; Williams, R. J. P. *The Biological Chemistry of the Elements*; Clarendon Press, Oxford University Press: Oxford, 1994.

(18) Frisch, M. J.; Trucks, G. W.; Schlegel, H. B.; et al. *Gaussian 98*, Revision A.6; Gaussian, Inc.: Pittsburgh, PA, 1998.

(19) Hoyau, S.; Ohanessian, G. *Chem. Phys. Lett.* **1997**, *280*, 266.

(20) Chuang, M.-C.; Folz, M. F.; Moore, C. B. *J. Chem. Phys.* **1987**, *87*, 3855.

(21) Green, W. H.; Morre, C. B.; Polik, W. F. *Annu. Rev. Phys. Chem.* **1992**, *43*, 591.

(22) Terentis, A. C.; Kable, S. H. *Chem. Phys. Lett.* **1996**, *258*, 626.

(23) Yamaguchi, Y.; Wesolowski, S. S.; Van Huis, T. J.; Schaefer, H. F. *J. Chem. Phys.* **1998**, *108*, 5281.